Structural and photoluminescence studies of Er implanted Be doped and undoped low-temperature grown GaAs

R. L. Maltez, Z. Liliental-Weber, J. Washburn, M. Behar, P. B. Klein, P. Specht, and E. R. Weber

Citation: Journal of Applied Physics **85**, 1105 (1999); doi: 10.1063/1.369236
View online: http://dx.doi.org/10.1063/1.369236
View Table of Contents: http://scitation.aip.org/content/aip/journal/jap/85/2?ver=pdfcov
Published by the AIP Publishing

Structural and photoluminescence studies of Er implanted Be doped and undoped low-temperature grown GaAs

R. L. Maltez,[a] Z. Liliental-Weber, and J. Washburn
Materials Science Division, Lawrence Berkeley National Laboratory, University of California, Berkeley, California 94720

M. Behar
Instituto de Física, UFRGS, Porto Alegre, RS, Brazil 91501-970

P. B. Klein
Naval Research Laboratory, Washington DC 20375-5347

P. Specht and E. R. Weber
University of California, Department of Material Science and Mineral Engineering, Berkeley, California 94720

(Received 31 August 1998; accepted for publication 13 October 1998)

Characteristic 1.54 μm Er^{3+} emission has been observed from Er-implanted and annealed, low-temperature grown GaAs Be doped and undoped samples. Er plateau implantations (480, 155, and 40 keV successive implants) were performed at 300 °C covering calculated Er concentrations from 10^{18} up to 10^{20} Er/cm^3. Cross-sectional transmission electron microscopy studies reveal very little structural damage for these elevated temperature implants up to an Er total fluence of 1.36×10^{14} Er/cm^2. No Er emission was observed from any of the as-implanted samples but it was observed after postimplantation annealings at 650 and 750 °C temperatures. The Er emission was significantly more intense after 650 °C anneals, for Be doped samples, and after 750 °C anneals for undoped samples. It appears on top of a broad background luminescence associated with midgap states. The Er emission intensity was found to scale linearly with the total Er implantation fluence up to Er concentration of $\sim 10^{19}$ Er/cm^3. Er precipitation was observed after 750 °C annealing for 10^{19} Er/cm^3 samples, but could be observed for 10^{20} Er/cm^3 Er-doped samples even after a 650 °C anneal. These precipitates are most likely ErAs. © *1999 American Institute of Physics.* [S0021-8979(99)07402-2]

I. INTRODUCTION

Rare earth (RE) elements have an incomplete $4f$ electronic shell that is screened from the outer crystalline environment by closed $5s^2$ and $5p^6$ orbitals. As a result, the transitions from a $4f$ excited state to the ground state retain essentially their atomic character, which means that RE doped materials characteristically exhibit sharp, temperature stable, and host independent luminescence spectra. For this reason, RE doped III–V semiconductors have potential application in semiconductor light-emitting diodes (LEDs), lasers, and as components for optical communication technology. In particular for the RE element Er, the internal transition from the first excited state to the ground state ($^4I_{13/2} \rightarrow {}^4I_{15/2}$) results in emission near 1.54 μm. This is an important wavelength because it corresponds to the minimum absorption in standard silica-based optical fibers.[1,2]

Such characteristic Er emission has already been observed for standard GaAs hosts doped with Er by different procedures, namely, liquid phase epitaxy (LPE),[3] molecular beam epitaxy (MBE),[4,5] metalorganic chemical vapor deposition (MOCVD),[6–8] and ion implantation.[2,9,10] In a previous work,[11] where we reported our first results, we have observed this Er emission for low temperature grown GaAs doped with Be (LT-GaAs:Be).

LT-GaAs[12] is a nonstoichiometric GaAs layer grown by MBE at much lower temperature (usually between 200 and 300 °C) than the standard 500–600 °C. Such layers have an arsenic excess around 1 at. %, which results in a high concentration of $(As)_{Ga}$ antisites as well as Ga vacancies. This high concentration of point defects leads to special characteristics for applications in high performance optoelectronic devices:[12,13] (i) high resistivity and breakdown strength; (ii) extremely short photoexcited carrier lifetime on the order of a few hundreds of femtoseconds.[12] However, because of this high concentration of point defects, Er photoluminescence (PL) was not necessarily expected in this material because these centers provide a very fast and efficient trapping channel to compete with the Er for the photoexcited carriers.

In addition, the doping with Be of LT-GaAs strongly suppresses As precipitation (as well as As out diffusion) upon annealing.[13] Be doped layers grown at ~300 °C show the same short photocarrier lifetime that is only obtained for undoped LT-GaAs grown at ~200 °C.[13] Thus, Be doping allows implantation up to 300 °C as well as postimplantation annealing with less risk of degrading the optical response.

One important point restricting the concentration of optically active Er sites is the Er solubility in the host material. It is generally accepted that Er atoms in precipitates would

[a]Postdoctoral fellowship by CAPES-Brasília/Brasil.

TABLE I. Implantation conditions employed to obtain the named samples 10^{18}, 10^{19}, and 10^{20} Er/cm^3. These implantation parameters were projected to result in an almost homogeneous Er concentration of 10^{18}, 10^{19}, and 10^{20} Er/cm^3, respectively, from 10 to 145 nm (plateau-like Er distributions).

Sample denomination	Implantation temperatures (°C)	Implantation energies (keV)	Implantation fluences (Er/cm^2)	Total implantation fluences (Er/cm^2)	GaAs types implanted
Plateau		480	9.4×10^{12}		
10^{18} Er/cm^3	300	155	3.1×10^{12}	1.36×10^{13}	LT-GaAs:Be
		40	1.1×10^{12}		
Plateau		480	9.4×10^{13}		LT-GaAs:Be
10^{19} Er/cm^3	300	155	3.1×10^{13}	1.36×10^{14}	LT-GaAs
		40	1.1×10^{13}		GaAs
Plateau		480	9.4×10^{14}		
10^{20} Er/cm^3	300	155	3.1×10^{14}	1.36×10^{15}	LT-GaAs:Be
		40	1.1×10^{14}		

not be optically active. The solubility of Er in LT-GaAs should therefore be taken into account to estimate the optimum Er doping concentration. Er solubility in standard GaAs was determined to be approximately 7×10^{17} Er/cm^3 by Poole *et al.*[14] They analyzed the incorporation of Er into GaAs layers during MBE growth by transmission electron microscopy (TEM). At higher concentrations, ErAs precipitates were formed. These precipitates had the rock salt structure and were completely coherent with the GaAs host.[14,15]

In our first work[11] we studied single and plateau-like Er implantations into LT-GaAs:Be (Er concentration was around 10^{19} Er/cm^3) performed at room temperature (RT) and at 300 °C temperature. It was verified that all samples implanted at 300 °C had an excellent crystalline quality as well as a considerably higher PL intensity than implants at RT.[11] We also showed that a postimplantation annealing was required to activate the Er emission, with the 650 °C anneals significantly more efficient than 750 °C anneals for LT-GaAs:Be.[11] This Er emission was found to occur on the top of a broad background luminescence. We also did not observe a clear Er precipitation even though the calculated Er concentration, in the samples, was typically one order of magnitude higher than the Er solubility limit determined by Poole *et al.*[14] In the present work we have studied the Er PL emission as a function of Er implanted concentration (and Er precipitation) as well as the evolution of the implantation damage with increasing Er fluence. In addition, we also have studied the Er PL behavior for undoped LT-GaAs. For this case, as will be shown, the characteristic Er emission shows a completely different dependence on the thermal treatment performed on the samples.

II. EXPERIMENTAL PROCEDURES

Undoped as well as Be doped ($[\mathrm{Be}]=7\times10^{19}$ cm^{-3}) LT-GaAs layers 1.5 μm thick were grown by molecular beam epitaxy on (001) GaAs substrates with a fixed As/Ga beam equivalent pressure ratio of 20. The GaAs substrate temperature during growth was 200 and 300 °C for the undoped LT-GaAs and Be doped LT-GaAs (LT-GaAs:Be), respectively. Plateau Er depth distributions were obtained by performing three consecutive Er implants at energies of 480, 155, and 40 keV, always keeping the sample at 300 °C temperature.

LT-GaAs:Be samples were implanted to different fluences in order to obtain three Er concentration levels along the plateau: (a) sample 10^{18} Er/cm^3 (the partial fluences for each of those energies were, respectively, of 9.4×10^{12}, 3.1×10^{12}, and 1.1×10^{12} Er/cm^2), (b) sample 10^{19} Er/cm^3 (the partial fluences were, respectively, 9.4×10^{13}, 3.1×10^{13}, and 1.1×10^{13} Er/cm^2); and (c) sample 10^{20} Er/cm^3 (the partial fluences were, respectively, 9.4×10^{14}, 3.1×10^{14}, and 1.1×10^{14} Er/cm^2). These implantation parameters were projected to result in an almost constant Er concentration of 10^{18} (case a), 10^{19} (case b), and 10^{20} Er/cm^3 (case c) from 10 to 145 nm, based on each individual profile as calculated by the TRIM[16] program. The named samples 10^{18}, 10^{19}, and 10^{20} Er/cm^3 were obtained by using **total** implantation fluences of 1.36×10^{13}, 1.36×10^{14}, and 1.36×10^{15} Er/cm^2, respectively. A summary of the implantation conditions is given in Table I.

The implantation carried out for the undoped LT-GaAs layers corresponds to case (b) above, i.e., $\sim10^{19}$ Er/cm^3 along the plateau. Also standard (and undoped) GaAs layers were Er implanted following the same case (b) condition to allow a direct comparison among the different GaAs types.

Rapid thermal annealings (RTA) for 30 s at 650 and 750 °C were performed on different pieces cleaved from each implanted sample. The structural quality of the layers was investigated using a Topcon 002B transmission electron microscope with 200 keV of acceleration voltage. Cross-sectional specimens were prepared by mechanical polishing and dimpling, followed by ion milling using a liquid nitrogen-cooled stage. Beam conditions 200, 400, and $0\bar{2}2$ for bright and dark field image modes were employed to obtain the micrographs.

PL measurements were performed at 10 K using 514 nm excitation from an argon ion laser. The emitted radiation was collected and analyzed with a 0.22 m double grating spectrometer, and the PL signal was detected by a liquid nitrogen-cooled germanium detector using standard synchronous detection techniques. A relatively wide spectral band-

pass of 3.4 nm was used for all of spectra, so that the weakest spectrum could still be observed and compared directly to the strongest. Some features, particularly for GaAs:Er annealed at 650 °C, exhibit a much smaller linewidth. The resolution of these features is not an important part of the present work.

The implantations were performed using the 500 kV ion implanter at the Instituto de Física, Porto Alegre. Annealing and transmission electron microscopy were performed at Lawrence Berkeley National Laboratory. The photoluminescence measurements were performed at the Naval Research Laboratory.

III. TEM MEASUREMENTS: RESULTS AND DISCUSSIONS

A. Concentration study

This study was made exclusively on LT-GaAs:Be samples. Figure 1 shows TEM micrographs from samples 10^{19} and 10^{20} Er/cm^3 before and after annealing. In this figure, pictures (a), (b), and (c) correspond to the 10^{19} Er/cm^3 samples and (d), (e), and (f) to the 10^{20} Er/cm^3 samples, i.e., same implants are on the same column. The first picture [(a) or (d)] is the observation from the as-implanted sample, the second picture [(b) or (e)] is after the 650 °C anneal and the last picture [(c) or (f)] is after the 750 °C anneal, i.e., same postimplantation histories are on the same row.

All the images in Fig. 1 are cross-sectional TEM micrographs in bright field (BF) taken with $\mathbf{g}=0\bar{2}\bar{2}$. The (001) surface is the sample edge located at the top of each figure. The BF $0\bar{2}\bar{2}$ image condition provides good contrast for damage observations. The main defects are dislocation loops. Due to the implantation at high temperature (300 °C) and the low total implantation fluence used, the 10^{18} Er/cm^3 sample does not show any visible damage, for either the as-implanted sample or after annealing. For this reason, TEM micrographs for this concentration are not present in Fig. 1. However, defects begin to be visible for 10^{19} Er/cm^3 samples.

Even for the higher Er concentrations 10^{19} and 10^{20} Er/cm^3, no visible defects could be observed for the as-implanted samples. The samples show very good crystalline quality from the point of view of extended defects [Figs. 1(a) and 1(d)]. These results suggest that even when the implantation fluence is increased by two orders of magnitude the great majority of the ion damage is being recovered during the implantation at 300 °C. This is in contrast to room temperature implants, where a significant amount of damage was observed in as-implanted material.[11]

Figures 1(b) and 1(e) are micrographs from samples annealed at 650 °C. The sample 10^{19} Er/cm^3 [Fig. 1(b)] still does not show evidence of significant damage while a strong damaged area can be noticed for the sample 10^{20} Er/cm^3 [Fig. 1(e)]. This damage is characterized by their dislocation loop densities (v_1) averaged from surface down to ~220 nm: 5×10^{-6} loops/nm^3, for sample 10^{19} Er/cm^3, and about 3×10^{-5} loops/nm^3, for sample 10^{20} Er/cm^3 [Fig. 1(e)]. The dislocation loop mean diameters ($\overline{2r}$) are ~1.5 nm and ~3.0 nm for those samples, respectively. However, even for the sample 10^{20} Er/cm^3, the near surface area (down to 75 nm) still keeps good crystalline quality. For this case, the high concentration of dislocation loops is restricted to the area of 75 to ~240 nm from the sample surface. This is the end of

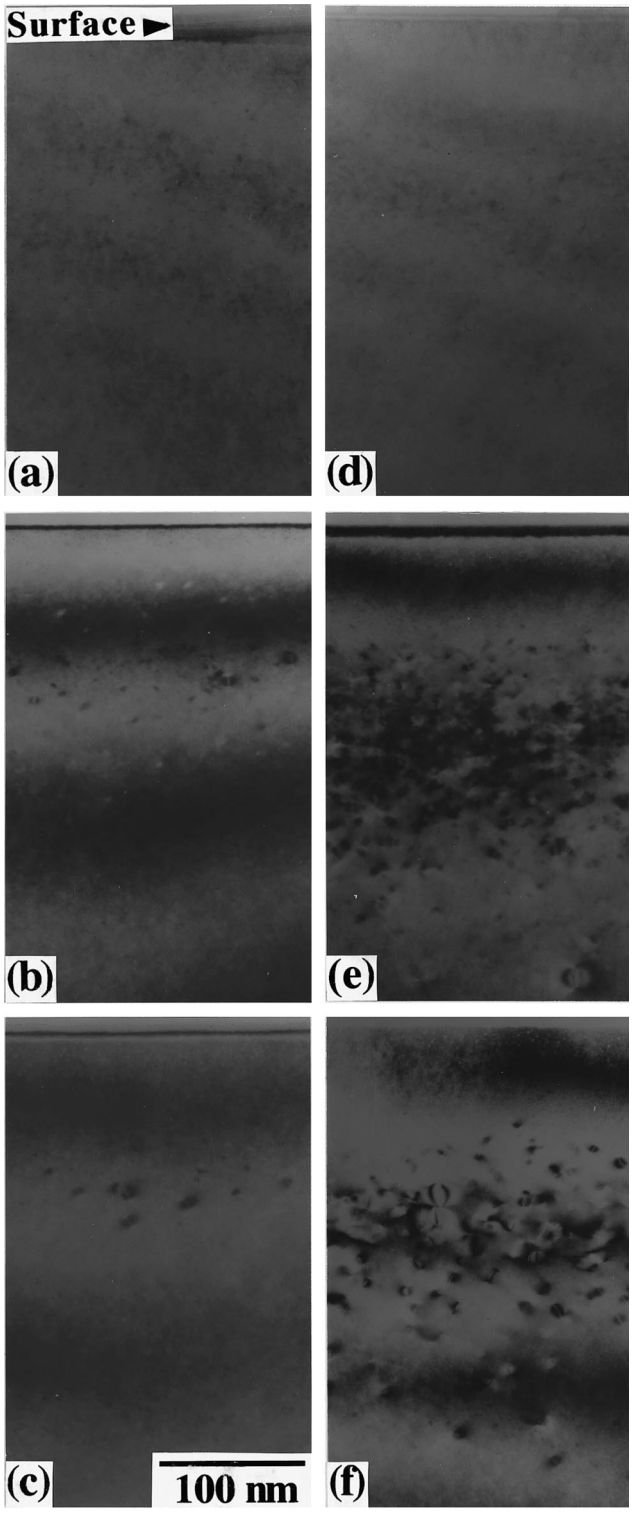

FIG. 1. Cross-sectional TEM micrographs (BF $0\bar{2}\bar{2}$) for plateau implanted samples at 300 °C. The (001) surface is at the top edge of each figure. Pictures (a), (b), and (c) correspond to the 10^{19} Er/cm^3 while (d), (e), and (f) correspond to the 10^{20} Er/cm^3 sample, i.e., the same implants are on the same column. For all of those cases the first picture (a) or (d) is the observation from the as-implanted sample, the second one (b) or (e) is after the 650 °C anneal and the last one (c) or (f) is after the 750 °C anneal, i.e., same postimplantation histories on the same row.

TABLE II. Estimates for the total extension of dislocation lines per unit volume of the sample.

RTA	10^{19} Er/cm^3, LT-GaAs:Be	$\overline{2r}\pi\nu_1$ (cm^{-2}) 10^{19} Er/cm^3, standard GaAs	10^{20} Er/cm^3, LT-GaAs:Be
650 °C	2.3×10^9	2.8×10^9	2.8×10^{10}
750 °C	2.2×10^9	2.9×10^9	3.1×10^{10}

range area since TRIM calculations indicate that the half height on the end of the Er plateau should be located around 145 nm. The near surface area (down to 75 nm) still keeps good crystalline quality.

Figures 1(c) and 1(f) are micrographs from samples annealed at 750 °C. It appears that small loops are annealed out for the sample 10^{19} Er/cm^3 [Fig. 1(c), $\upsilon_1=2\times10^{-6}$ loops/nm^3], but still some small loops ($\overline{2r}\sim3.5$ nm) appear around 120 nm (end of range area). However, there is no drastic change for the sample 10^{20} Er/cm^3, it keeps essentially the same depth damage distribution with just a little lower loop density ($\upsilon_1=2\times10^{-5}$ loops/nm^3) than observed after the 650 °C anneal. The main difference is that the dislocation loops now seem to have a more homogeneous and larger size ($\overline{2r}\sim5$ nm). Also the transition between the clean area (near surface) and the end of range area is a little deeper than before (about 90 nm depth).

Table II shows estimates, from TEM micrographs, for the quantity $\overline{2r}\pi\upsilon_1$, which represents the total length of dislocation lines per unit volume. This factor estimates the crystalline quality of the implanted area from the point of view of extended defects (averaged from surface down to ~220 nm). The values for sample 10^{20} Er/cm^3 (implanted at 300 °C) are in the same range as observed for room temperature (RT) implants.[11] However, the total implantation fluence for this 300 °C implanted sample is about 25 times higher than that employed for the RT implant.[11]

B. Material type study

This study was made on 10^{19} Er/cm^3 Er implanted samples. The evolution of the structural damage for LT-GaAs:Be was reported in the previous section with analyses of Figs. 1(a)–1(c). Also it is clear, from those figures, that arsenic precipitation in those samples was strongly suppressed due to the Be doping. The high temperature implantation did not interfere with this suppression. Some very small As precipitates for Be doped samples are seen more clearly after annealing at 750 °C. Double black lobes (characteristic of small As precipitates) can be seen beyond the implanted area.

This strong suppression of As precipitation obtained by Be doping is more clearly evident when we compare the image from a Be doped sample to an undoped LT-GaAs sample, as shown in Fig. 2. In this figure, cross-sectional TEM images from a Be doped LT-GaAs sample [Fig. 2(a)] and from a standard GaAs sample [Fig. 2(b)] are compared to that from the undoped LT-GaAs sample [Fig. 2(c)]. All of them are 10^{19} Er/cm^3 implanted samples annealed at 650 °C. Two strong differences can be seen for the undoped LT-GaAs [Fig. 2(c)]: there is a very intense As precipitation and a complete absence of ion implantation damage. The average diameter of the As precipitates is about 5 nm after the 650 °C annealing [Fig. 2(c)]. The undoped sample annealed at 750 °C shows larger As precipitates (~9 nm in diameter) and again no implantation damage was observed. Only the undoped as-implanted sample shows a faint indication of damage, very similar to that observed in Figs. 1(a) and 1(d). The complete absence of extended defects is a surprising characteristic that may be correlated to the strong As precipitation observed for undoped samples. Standard GaAs also was analyzed and shows damage levels very similar to those observed for the Be doped case (see Table II for estimates).

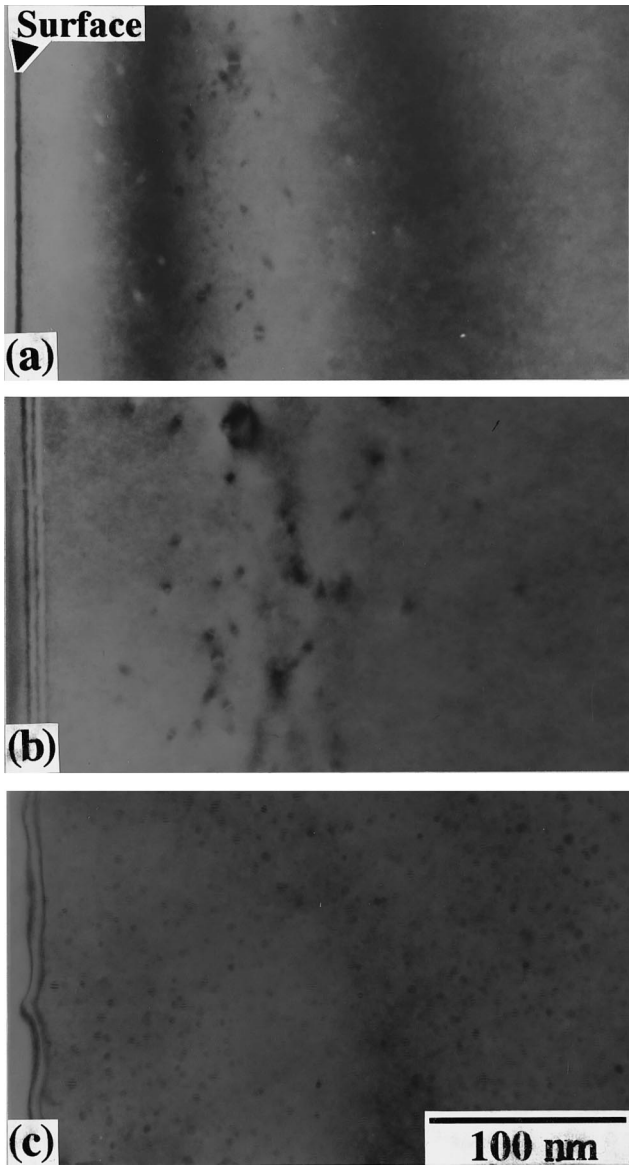

FIG. 2. Cross-sectional TEM micrographs (BF $0\overline{2}2$) for 10^{19} Er/cm^3 plateau implantation at 300 °C after annealing at 650 °C. Picture (a) corresponds to the LT-GaAs sample doped with Be, picture (b) to the standard GaAs sample, and picture (c) to the undoped LT-GaAs sample. The (001) surface is at the left edge of each figure.

C. ErAs precipitation

Within the implanted area, after annealing, a different type of precipitate was observed from contrast analysis under

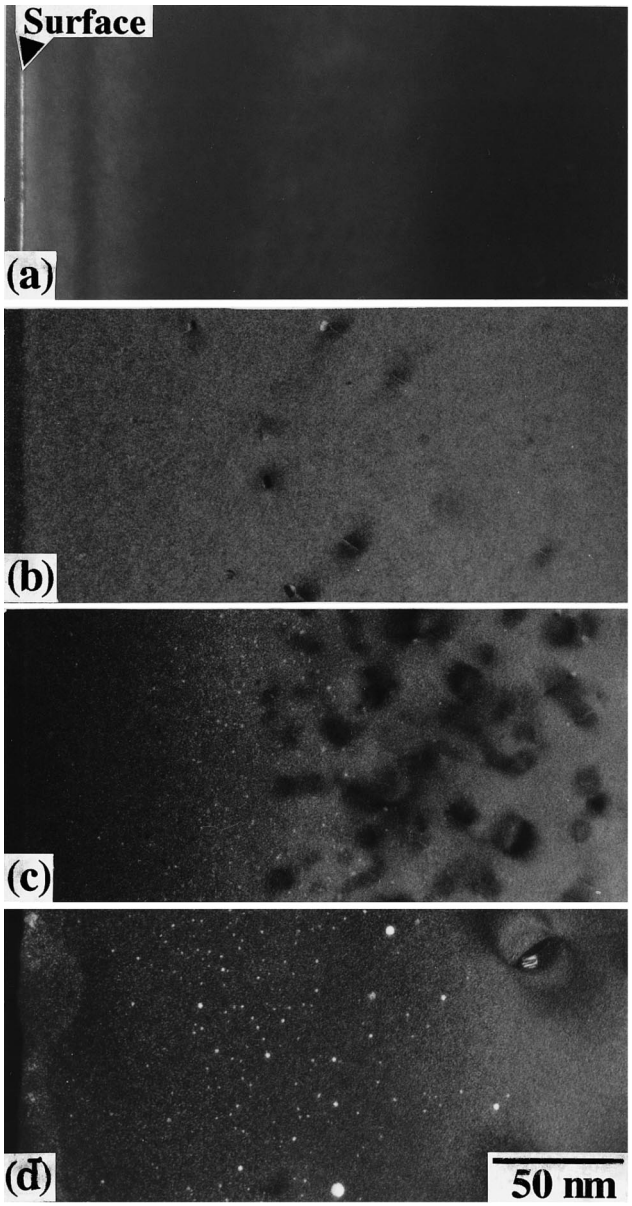

FIG. 3. Cross-sectional TEM micrographs for DF 200 condition where the (001) surface is at the edge on the left of each figure. (a)–(c) Correspond to the 10^{18}, 10^{19}, and 10^{20} Er/cm^3 plateau implanted samples, respectively. All of them are after RTA annealing at 750 °C for 30 s. (d) Corresponds to a special annealing at 800 °C for a half hour performed on 10^{20} Er/cm^3 plateau implanted sample.

dark field image conditions taken with $\mathbf{g}=200$. Figure 3(d) is an example of this special precipitation. The images in Fig. 3 are cross-sectional TEM micrographs in DF 200. The (001) surface is at the left edge of each figure. Figures 3(a)–3(c) correspond to the Be doped samples 10^{18}, 10^{19}, and 10^{20} Er/cm^3, respectively, after annealing at 750 °C for 30 s. Figure 3(d) corresponds to a special annealing at 800 °C for a half hour performed on the 10^{20} Er/cm^3 Be doped sample. The purpose of this annealing was to obtain a more clear precipitation.

As mentioned before, these sharper and bright precipitates can be seen just within the implanted area and their number increases with increasing Er concentration. For the sample 10^{18} Er/cm^3 there is no such precipitation [see Fig. 3(a)]. This can be understood taking into account that the Er solubility is around 7×10^{17} Er/cm^3 in standard GaAs, reported by Poole *et al.*[14] The 10^{19} Er/cm^3 plateau implanted samples show these precipitates, but only after annealing at 750 °C and particularly at dislocation cores [Fig. 3(b)]. The highest concentration analyzed was 10^{20} Er/cm^3 [Fig. 3(c)]. It shows a high concentration of bright dots from the surface down to around 150 nm that agrees fairly well with the end of the Er depth profile as calculated by the TRIM program.[16] Also seen from Fig. 3(c) is a decrease in their number in the area where dislocation loops are present, with a simultaneous increase in their sizes. This could be expected since the Er concentration must be approximately the same down to around 145 nm. In the near surface area (down to 90 nm) these bright precipitates show an average size around 1 nm in diameter but it increases to around 1.5 nm between 90 and 150 nm. The same argument can explain why we see larger precipitates in the sample 10^{19} Er/cm^3. Fewer active Er nucleation centers can be expected due to the lower Er concentration. These centers are mainly the dislocation cores that also are present at lower density compared to the sample 10^{20} Er/cm^3.

Longer annealing at higher temperature, done on the sample with the highest Er concentration (10^{20} Er/cm^3), makes this Er precipitation clear [see Fig. 3(d)]. Particularly in this figure, larger precipitates ($\sim$4 nm in diameter) can be seen in the end of range area. It is also likely that some longer range Er diffusion has occurred for this case, since precipitates can now be seen deeper into the sample. Another interesting point is the different contrast observed on DF 200 micrographs for precipitates very deep in the sample where no Er could be found. These are clearly As precipitates and show very faint dark contrast (and not bright) for this image condition.

Er precipitation is not observed for any of the as-implanted samples. After the annealing at 650 °C, just the 10^{20} Er/cm^3 sample shows this bright dot contrast but less intense than observed after 750 °C annealing [Fig. 3(c)]. The other GaAs types also do not show any indication of this precipitation in the as-implanted samples. The LT undoped GaAs (10^{19} Er/cm^3 sample) does not show this kind of contrast for any annealed sample either. This is consistent with the fact that we did not observe dislocation loops for these undoped samples, as were observed for Be doped samples. The analyses done on the standard GaAs (10^{19} Er/cm^3 sample) show a few bright dots (less than the ones observed in the Be doped case) after annealing at 750 °C. We have also analyzed unimplanted samples submitted to the same annealing conditions and they have not shown any evidence of this kind of contrast under DF 200.

All these observations, concerning sharp bright contrast for DF 200 for some precipitates exclusively in the implanted area, suggest that ErAs precipitation is occurring in these cases. These precipitates would have the rock salt structure and could be completely coherent with the GaAs host. In this case, ErAs precipitates, $a_0=5.732$ Å, would be slightly compressed in order to be accommodated into the GaAs or LT-GaAs matrices, $a_0=5.653-5.659$ Å. This possibility of formation of ErAs precipitates has also been re-

ported for standard GaAs[14] and subsequently confirmed by channeling measurements.[15] These precipitates appear as bright spots under DF 200 due to their structure factor which is much greater than that of the surrounding GaAs lattice. High resolution images of these precipitates indeed confirm that they are completely coherent with the matrix. Because they have almost the same lattice parameter as the GaAs lattice and are completely coherent, extra spots could not be observed on the diffraction pattern.

In our case, the ion implantation procedure incorporates Er into LT-GaAs as a supersaturated solid solution: none of the as-implanted samples show ErAs formation; it can be observed only after annealing at 750 °C for samples with an Er concentration $\sim 10^{19}$ Er/cm^3; for this kind of precipitation to be observed after annealing at 650 °C, an Er concentration around 10^{20} Er/cm^3 (2 orders of the magnitude higher than the estimated limit of solubility) is required. The supersaturated condition persists after annealing probably because, Er diffusion in the LT-GaAs host is not fast enough during RTA annealings, or the temperatures were not high enough for precipitate nucleation. This is in agreement with the observation that precipitation begins to occur first at dislocation cores for the 10^{19} Er/cm^3 sample [Fig. 3(b)] and that longer annealings and higher temperatures can increase the ErAs precipitation, as observed in Fig. 3(d).

IV. PHOTOLUMINESCENCE MEASUREMENTS: RESULTS AND DISCUSSIONS

Figure 4 shows PL spectra comparing results from LT-GaAs:Be plateau implanted samples with different Er concentrations, namely, 10^{18} [Fig. 4(a)], 10^{19} [Fig. 4(b)], and 10^{20} Er/cm^3 [Fig. 4(c)]. The measurements were performed on as-implanted, annealed at 650 and 750 °C samples, resulting in three spectra for each concentration. As can be seen from this figure, the emission in that spectral range is dominated by a broad background signal (except for the 10^{20} Er/cm^3 sample annealed at 650 °C). This background, shown in the insert in Fig. 4(c) for the 10^{19} Er/cm^3 sample annealed at 650 °C, results from a very broad emission that appears to peak near 1500 nm, due to the long wavelength cutoff of the Ge detector. The broad background PL is observed to increase monotonically with increasing anneal temperature, with elevated implantation temperature,[11] and with decreasing damage as seen by TEM. These observations suggest that the observed intensity increase is associated with the improvement in crystal quality due to reduction of residual implantation damage. This broad emission is observed for all of the samples studied here, including the standard GaAs material. Low temperature photoluminescence measurements of this band were carried out using a liquid nitrogen cooled PbS detector (1–3.6 μm response) in order to measure the complete spectrum for this feature. The background PL of the plateau-implanted samples shown in Fig. 4 was found to be due to a very broad emission ($\sim$1.1–2.5 μm) resulting from the superposition of two emission bands: one centered at $\sim$0.65 eV and the other centered at $\sim$0.8 eV. The latter emission band is primarily responsible for the broad background upon which the Er PL is observed [inset, Fig. 4(c)] as well as for the long high energy tail reaching

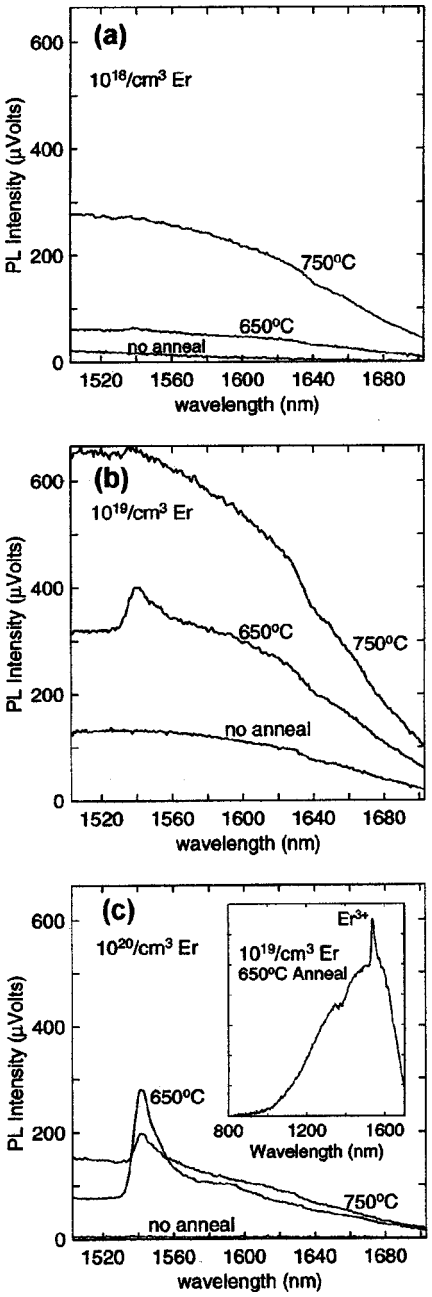

FIG. 4. PL spectra comparing plateau implanted samples at 300 °C, namely, 10^{18} (a), 10^{19} (b), and 10^{20} Er/cm^3 (c). Spectra are shown for the as-implanted, annealed at 650 and 750 °C samples, resulting in three spectra for each implantation condition. Insert in (c): Er emission, from 10^{19} Er/cm^3 sample annealed at 650 °C, on top of the broad background PL shown over an extended wavelength range.

almost to the band gap. These bands are both commonly observed from liquid encapsulated Czochralski (LEC)-grown bulk GaAs, the 0.65 eV band originating from transitions between the EL2 antisite-related defect and both band edges,[17] while the 0.8 eV band is associated with the presence of microdefects (precipitates, vacancy complexes, dislocation loops).[18]

A distinct feature in Fig. 4 is the 1.54 μm Er emission. As reported in previous work,[11] the as-implanted samples do not show any sign of this Er emission in any case. It is unlikely under these conditions that much of the Er was in

optically active sites, and the carrier lifetimes were presumably also very short, due to the large amount of damage induced by the implantation of heavy ions. It is presently not possible to determine which of these two effects is dominant. It is also noteworthy that in the spectrum shown in the insert in Fig. 4(c), there is no evidence of any band edge emission. This suggests that the carrier lifetime in the Er-implanted and annealed material is still relatively short.

The optimum annealing temperature seems to be around 650 °C (the Er emission strongly decreases after annealing at 750 °C), showing a temperature behavior similar to that observed for standard GaAs:Er samples.[1] This behavior strongly suggests that the optically active Er site is being thermally destabilized into a ''dark site.'' This is similar to the activation and destabilization of Er^{3+} sites with anneal temperature observed in Er-implanted GaAs.[9] In previous work[11] we showed that in annealed samples the Er PL intensity varies linearly with implantation fluence, up to an Er concentration of about 10^{19} Er/cm^3. This is also reflected by the data in Fig. 4, as the 10^{18} and 10^{19} Er/cm^3 plateau implants exhibit a similar linear increase of the Er emission intensity with Er implantation fluence. However, between 10^{19} and 10^{20} Er/cm^3 the emission intensity is seen in Fig. 4 to rise only a factor of 2.4, indicating a transition to sublinear behavior that would suggest a saturation at higher concentrations. At higher concentrations a smaller fraction of the total amount of the implanted Er would be expected to find optically active sites. This can result from the formation of Er complexes or ErAs precipitates.

Figure 5 shows PL spectra comparing results from all of the three GaAs material types studied, i.e., Be doped [Fig. 5(a)] and undoped LT-GaAs [Fig. 5(b)] as well as the standard GaAs [Fig. 5(c)] used as reference. The figure also exhibits the evolution of the PL spectra as a function of anneal temperature. Postimplantation annealing was found necessary to optically activate the implanted Er in all three types of GaAs materials. After the 650 °C anneal, the standard GaAs shows a highly structured spectrum that represents a different Er site than that observed in LT-GaAs. The standard GaAs also shows a more intense Er emission, since this material has a much lower concentration of point defects which can act as trapping centers for the photocarriers and thus compete with the Er radiative centers. Upon annealing at higher temperature (750 °C) the Er emission in standard GaAs changes line shape to one that is similar to that in LT-GaAs, characterized by a single broad PL peak that would suggest an element of randomness in the environment of the Er site. Variation in the Er environment would cause a smearing of the crystal field splittings of individual Er^{3+} levels, leading to such a broadened line shape. The site associated with this Er emission peak is the only one that is observed (by its spectral signature) in Er-implanted LT-GaAs prepared over a wide range of implantation, annealing, and doping conditions. Presumably, it is the only site that can trap carriers fast enough to compete with the trapping at other defects sites inherent to the low-temperature grown material.

It is significant that the dependence of the Er emission intensity on anneal temperature for Be-doped LT-GaAs [Fig. 5(a)] is distinctly different than that for undoped LT-GaAs samples [Fig. 5(b)]. For the latter material, the Er emission from the 750 °C annealed sample was observed to be [Fig. 5(b)] almost twice the intensity of the 650 °C annealed sample, i.e., the optimum anneal temperature is near or greater than 750 °C, and not the same as for the others materials. Since the Er PL intensity peaks near 650 °C for both Be-doped LT-GaAs [Fig. 5(a)] and standard GaAs [Fig. 5(c)], the distinct dependence with anneal temperature in the undoped LT-GaAs cannot be directly related to the lack of Be doping. We believe that this behavior derives from the fact that the short carrier lifetimes of Be-doped LT-GaAs are more stable during annealing than those of undoped LT-GaAs.[13] Thus, the longer carrier lifetimes of the undoped

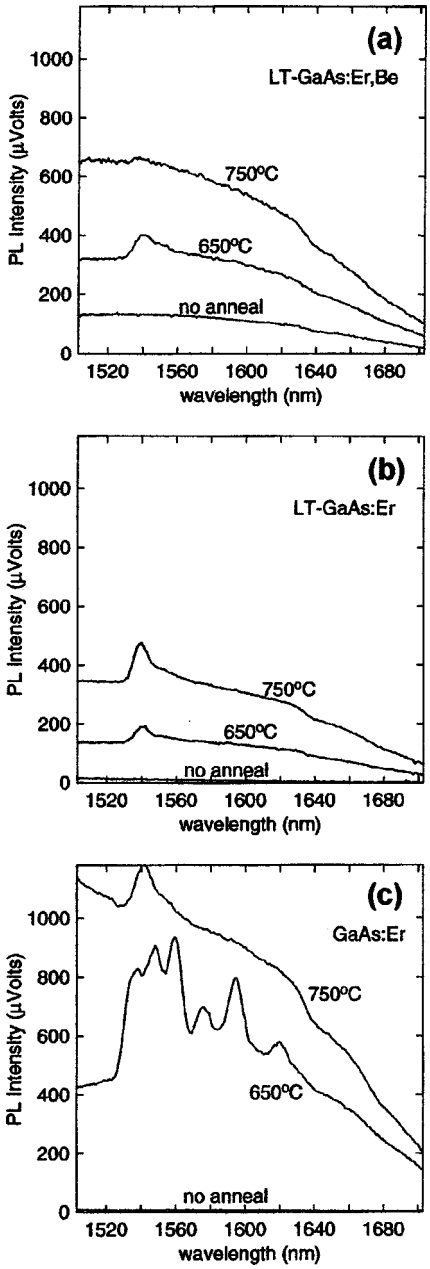

FIG. 5. PL spectra from 10^{19} Er/cm^3 samples comparing different material types: LT-GaAs:Be (a), undoped LT-GaAs (b), and standard GaAs (c). Spectra are shown for the as-implanted, 650 and 750 °C annealed samples, resulting in three spectra for each material type.

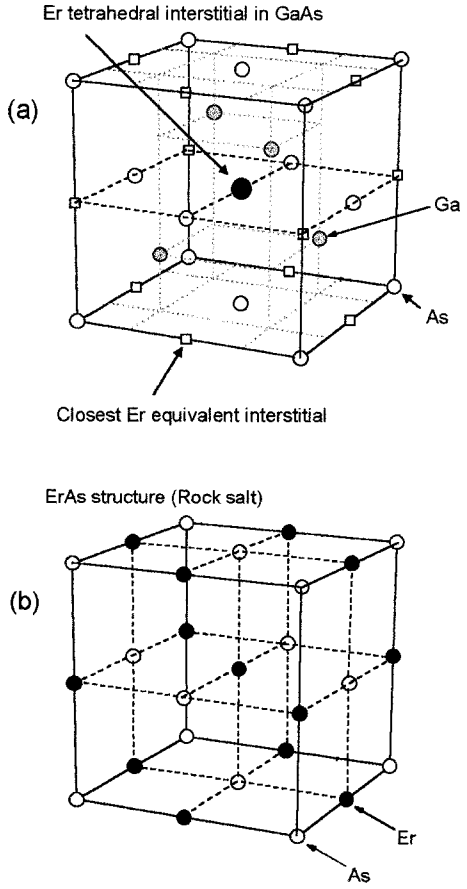

FIG. 6. (a) GaAs structure (Zinc blende; $a_0 = 5.653$ Å) with an Er atom (full circle) occupying the tetrahedral interstitial site (supposedly the Er optically active site in LT-GaAs). Also shown as squares the nearest equivalent tetrahedral interstitial sites. (b) ErAs structure (rock salt; $a_0 = 5.732$ Å).

samples annealed at 750 °C can enhance the probability of photoexcited carriers being trapped at Er radiative centers, resulting in more intense Er PL, even though the concentration of these centers may have decreased during the anneal in a manner similar to that in the Be-doped samples.

Finally some speculation about the likely optically active center can be made comparing TEM and PL results. The optically active center in GaAs has been suggested to be the Er tetrahedral interstitial site.[9,5,19] As noted earlier, the strong decrease in the 1.54 μm Er emission observed after 750 °C annealing for LT-GaAs:Be and standard GaAs indicates that the optically active Er sites are becoming thermally unstable. We also begin to observe some ErAs precipitation at this annealing temperature. These two observations suggest the possibility that, at increasingly higher anneal temperatures, instead of having a high concentration of isolated Er interstitials in the GaAs matrix, we now have a high concentration of ''Er–As complexes.'' For example, these Er–As complexes could be clusters of Er associated with clusters of the Ga vacancies, which are common in LT-GaAs materials. The specific isolated Er tetrahedral interstitial site considered here is that represented by the full black circle in Fig. 6(a), which shows the GaAs unit cell. In this figure the locations of the nearest equivalent interstitial sites are shown as square symbols. For comparison, the rock salt structure of ErAs is shown in Fig. 6(b). The ErAs structure can be seen as the limit of the structure in Fig. 6(a) with all the Er tetrahedral interstitials being effectively occupied by Er atoms and all the Ga sites vacant. From this point of view, the Er–As complexes could be the initial step for ErAs precipitation. The following three facts support this picture: Er tetrahedral interstitial sites are a natural precursor for ErAs precipitation;[15] Er was incorporated into the matrix as a supersaturated solution;[14] and a sublinear relationship between the Er emission intensity and the total implantation fluence was observed for the sample with the highest Er concentration.

V. CONCLUSIONS

In this work we have studied the characteristic Er emission, the crystalline quality and the Er precipitation of Er implanted Be doped and undoped LT-GaAs samples. We have shown that it is possible to obtain the 1.54 μm Er emission in LT-GaAs samples. This suggests that the carrier trapping time at the Er site is relatively short. The optimum annealing temperature for Er activation is around 650 °C (or lower) for LT-GaAs:Be, and around 750 °C (or higher) for undoped LT-GaAs. We conclude that this different thermal behavior for the undoped material is due to the degradation of the ultrashort carrier lifetime for 750 °C annealing in this material. TEM measurements clearly show that samples implanted at 300 °C have excellent crystalline quality up to the total fluence of 1.36×10^{14} Er/cm^2 (10^{19} Er/cm^3 plateau samples). The damage recovery of the undoped material is even better and does not show any evidence of extended defects, but does show an intense As precipitation. We have also observed that ion implantation is able to incorporate Er into the matrix as a supersaturated solid solution. This supersaturated state appears to be metastable, at least up to an annealing temperature of 650 °C (for 30 s) and for Er concentrations below $\cong 10^{19}$ Er/cm^3. Precipitates showing good contrast on DF 200 have been observed exclusively within the implanted area after annealing. They probably are ErAs precipitates with the rock-salt structure. This work also suggests that even higher Er PL intensity could be obtained by performing Er implants to higher fluences.

ACKNOWLEDGMENTS

This research was supported by AFOSR-ISSA-90-0009. R. L. Maltez work was also supported by CAPES-Brasilia/ Brasil postdoctoral fellowship. The use of facilities of the National Center for Electron Microscopy at Lawrence Berkeley National Laboratory, supported by the U.S. Department of Energy under Contract No. DE-AC03-76SF00098, is very much appreciated.

[1] G. S. Pomrenke, H. Ennen, and W. Haydl, J. Appl. Phys. **59**, 601 (1986).
[2] A. Polman, J. Appl. Phys. **82**, 1 (1997).
[3] F. Bantien, E. Bauser, and J. Weber, J. Appl. Phys. **61**, 2803 (1987).
[4] R. S. Smith, H. D. Muller, H. Ennen, P. Wennekers, and M. Maier, Appl. Phys. Lett. **50**, 49 (1987).
[5] D. W. Elsaesser, J. E. Colon, Y. K. Yeo, R. L. Hengehold, K. R. Evans, and J. S. Solomon, J. Cryst. Growth **127**, 707 (1993).
[6] K. Uwai, H. Nakagome, and K. Takahei, J. Cryst. Growth **93**, 583 (1988).
[7] J. Nakata, M. Taniguchi, and K. Takahei, Appl. Phys. Lett. **61**, 2665 (1992).

[8] K. Takahei, A. Taguchi, Y. Horikoshi, and J. Nakata, J. Appl. Phys. **76**, 4332 (1994).
[9] P. B. Klein, F. G. Moore, and H. B. Dietrich, Appl. Phys. Lett. **58**, 502 (1991).
[10] A. Kozanecki, M. Chan, C. Jeynes, B. Sealy, and K. Homewood, Solid State Commun. **78**, 763 (1991).
[11] R. L. Maltez, Z. Liliental-Weber, J. Washburn, M. Behar, P. B. Klein, P. Specht, and E. R. Weber, Appl. Phys. Lett. **73**, 2170 (1998).
[12] G. L. Witt, R. Calawa, U. Mishra, and E. Weber, Mater. Res. Soc. Symp. Proc. **241**, (1991); F. W. Smith, *ibid.* **241**, 3 (1991).
[13] P. Specht, S. Jeong, H. Sohn, M. Luysberg, A. Prasad, J. Gebauer, R. Krause-Rehberg, and E. R. Weber, International Conference on Defects in Semiconductors Proceedings, ICDS 19, Aveiro, Portugal, 1997, Mat. Sci. Forum, Part 2 **258–263**, 951 (1997).
[14] I. Poole, K. E. Singer, and A. R. Peaker, J. Cryst. Growth **121**, 121 (1992).
[15] J. Nakata, N. Jourdan, H. Yamaguchi, K. Takahei, Y. Yamamoto, and Y. Kido, J. Appl. Phys. **77**, 3095 (1995).
[16] J. F. Ziegler, J. P. Biersack, and U. Littmark, *The Stopping and Range of Ions in Solids*, (Pergamon Press, Oxford, 1985), Vol. 1.
[17] M. Tajima, Jpn. J. Appl. Phys., Part 2 **21**, L227 (1982).
[18] M. Tajima, Jpn. J. Appl. Phys., Part 2 **26**, L885 (1987), and references therein.
[19] E. Alves, M. F. da Silva, K. R. Evans, C. R. Jones, A. A. Melo, and J. C. Soares, Nucl. Instrum. Methods **B80/81**, 180 (1993).